Lung Nodule Segmentation and Detection in Computed Tomography

Salsabil Amin El-Regaily
Basic Science Department at the Faculy of Computer and Information Sciences
Ain Shams University
Cairo, Egypt
salsabil_amin@cis.asu.edu.eg , salsabil.amin@gmail.com

Mohammed Abdel Megeed Salem
Scientific Computing Department at the Faculty of Computer and Information Sciences
Ain Shams University
Cairo, Egypt
salem@cis.asu.edu.eg ,*German University in Cairo, GUC,*
Faculty of Media Engineering & Technology
mohammed.salem@guc.edu.eg

Mohamed Hassan Abdel Aziz
Basic Science Department at the Faculy of Computer and Information Sciences
Ain Shams University
Cairo, Egypt
Mohamed.Hassan@cis.asu.edu.eg

Mohamed Ismail Roushdy
Computer Science Department at the Faculy of Computer and Information Sciences)
Ain Shams University
Cairo, Egypt
mroushdy@cis.asu.edu.eg

***Abstract*— Computer Aided Detection (CAD) systems provide a second opinion to radiologists in detecting lung cancer by providing automated analysis of the scans. The proposed CAD system consists of five processing steps: image acquisition, pre-processing, lung segmentation, nodule detection and false positive reduction. First, 400 CT scans are downloaded from the Lung Image Database Consortium (LIDC). Preprocessing is implemented using contrast stretching and enhancing. Lung segmentation and nodule detection stages are performed using a combination of region growing, thresholding and morphological operations. Each 3D structure is then subjected to tabular structure elimination to provide nodule candidates. In the false positive reduction stage, some of the basic nodule features are extracted from the training data to set thresholds for a simple rule-based classifier. The CAD achieved sensitivity of 77.77%, specificity of 69.5% and accuracy 70.53 % with an average 4.1 FPs/scan.**

Keywords—Lung Cancer, Computer Aided Detection, Computed Tomography, Segmentation, Rule-Based Classifier

I. INTRODUCTION

One of the primary causes of death in the world is Lung cancer [1]. Pulmonary nodules are caused by the uncontrollable irregular growth of cells in the lung parenchyma. Detecting these nodules in the lung tissue in an early phase increases the chances of survival for the patient and improves efficiency of the treatment [2]. Lung nodules are spherical abnormalities with a diameter of up to approximately 30mm [3]. One of the most accurate screening methods for detecting lung nodules is computed tomography (CT) scans. The whole chest can be scanned in a few seconds using multi-detector row CT scanners. These scanners provide high quality scans with isotropic voxels. CT scans can show the density difference between normal and diseased tissue. Also, CT makes it possible to detect the small or ground-glass nodules that can be hardly seen in the other medical imaging techniques, like chest radiography [4]. However, making an accurate diagnosis based on analyzing the CT scans alone can be a very challenging and time-consuming task, as a CT scan could contain between 150-500 slices that must be checked by a radiologist [5]. As a result, many CAD methods are developed for automated lung nodule detection to provide a second opinion to the radiologists and help them make a more accurate diagnosis in a short amount of time. Also, human experts may miss subtle important details that could be located by automated CAD systems [6].

Detection of lung nodules can be a very difficult task as it is hard to differentiate between the lung internal structure and the nodules, especially if the nodule is attached to the lung wall or to the end of a vessel. Also, the size of nodules can vary significantly. This paper proposes a technique to face these challenges and recognize the differences between spherical nodules and internal tabular structure of the lung. It can also handle the cases in which the nodule is attached to the chest wall or connected to the blood tree. The work is totally automated without required external interference, and produces consistent results with the same output for the same input.

The paper is organized as follows: section 2 presents related work to the topic of lung cancer detection in CT scan in 2D or 3D spaces. Section 3 describes the details of the proposed scheme. Section 4 presents results and discussion.

II. RELATED WORK

This section provides an overview of some of the state-of-art techniques used for detecting lung nodules in computed tomography. There exist a number of review papers on lung nodule segmentation and detection [7]–[15].

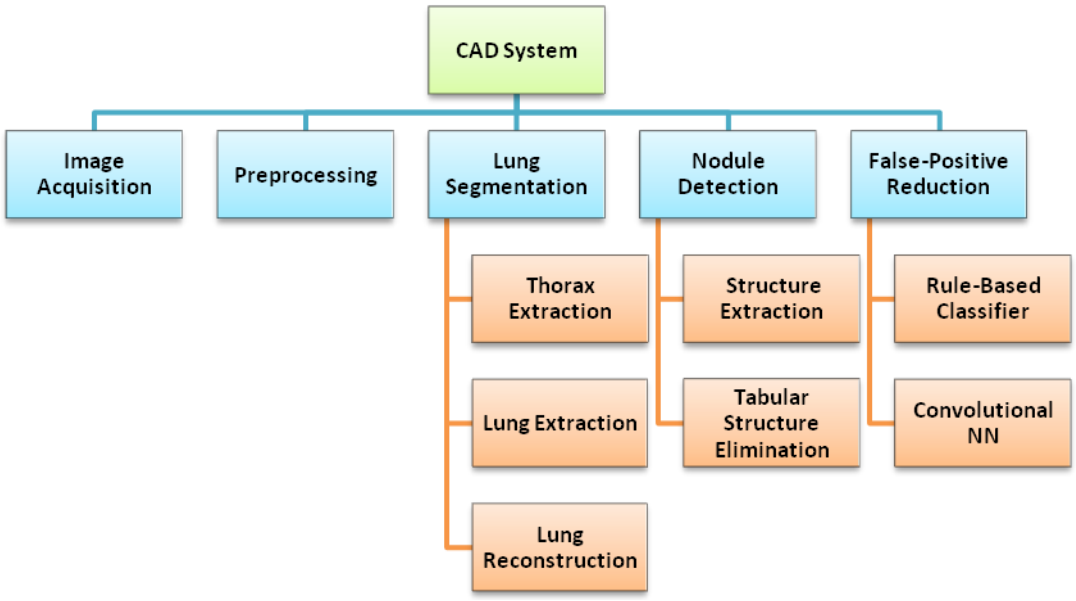

Fig. 1 Simple chart of the proposed methodology

Messay, et al. [16] used thresholding followed by 2D morphological analysis and a rule-based analysis to identify the lungs and detect the nodules. Then a Support Vector Machine (SVM) based on Radial Basis Function (RBF) is used to reduce the number of false positives. Tan, et al. [17] applied multi-thresholding to segment the lungs then calculated the maxima of the normalized gradient in 3D to generate seed points for nodule clusters. Fantacci, et al. [18] utilized a wavefront algorithm and morphological closing to define the inner surface of the lungs. Then a Blob-detection algorithm based on multi-scale and Gaussian filtering is used to detect nodule candidates. Ye, et al. [19] proposed a 3D adaptive fuzzy thresholding method that obtained the initial lung mask. Then antigeometric diffusion model followed by volumetric shape index is used to differentiate spherical objects from oblong vessels. Finally, a MEM-Based segmentation was carried out to iteratively estimate the model parameters and calculate each voxel probability. Kuppusamy, et al. [20] used Ant Colony Optimization (ACO) to detect the edges and then the output was fed to a black circular neighborhood algorithm. The output of this phase was the center of the detected nodules. De Carvalho, et al. [21] used Genetic Algorithm (GA) to select the best model and features, followed by a SVM for classification. Abduh, et al. [22] defined small windows for each ROI to calculate features, then a stepwise feature selection (SFS) algorithm was utilized to filter the best features which were used as an input to K-Nearest Neighbor (KNN) and SVM classifiers. . In the study by Dou, et al. [23] a simple strategy to encode multi-level contextual information with Convolutional Neural Networks (CNNs) was proposed, which could handle lung nodules of different sizes and shapes effectively. Three deep learning models were constructed by Sun, et al. [24] : CNN, Deep Belief Networks (DBNs) and Stacked Denoising Autoencoder (SDAE). The three models were tested and compared to the traditional CAD systems, and DBNs achieved the highest accuracy. Duggan, et al. [25] utilized Active Contour Model to extract the lung structure with similar intensity values into one big volume. Then Connected Component Labeling was used to separate them followed by a Rule-based classifier to reduce the numbers of false positives.

III. METHODOLGY

This section presents the proposed method for lung segmentation and nodule detection in detail through the following subsections as explained in Fig. 1.

A. Image Acquisition

Image acquisition is the process of acquiring medical images from imaging modalities. There are several lung screening techniques, among which the CT has more advantages, as it allows screening the whole lung area with higher contrast and better details. The Lung Image Database Consortium (LIDC) provided by the National Cancer Institute (NCI) is one of the largest public databases available [26]–[28]. LIDC is the fully annotated by four different radiologists. The observations are done on two consecutive phases: first the blinded phase, then the un-blinded one where each observer could see the results of the other three observers. This database shows the location of the nodules along with their characteristics such as subtlety, solidity, spiculation, lobulation, sphericity in XML files within each scan. The dataset is an international web-available resource, hosted by the National Biomedical Imaging Archive (NBIA, https://imaging.nci.nih.gov/ ncia/login.jsf).

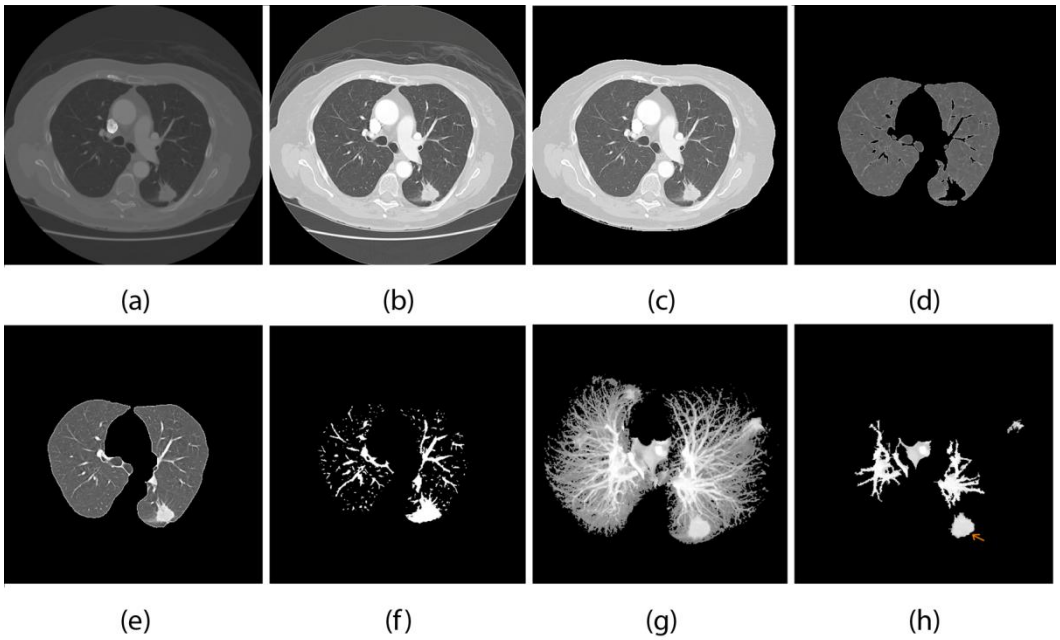

Fig. 2. Proposed CAD sequence (a) Original slice (b) Result of the preprocessing step with higher contrast (c) Thorax extraction results with the external areas removed (d) Lung extraction output after the removal of the thoracic wall with holes and obvious errors (e) Reconstructed lungs using morphological processing (f) Internal structure as appears in a 2D slice after thresholding (g) Result of 3D Region Growing (h) Result of tabular structure elimination with most of the vessels removed. The actual nodule is pointed at with an orange arrow in the bottom right corner of the image

Total of 400 cases are downloaded for this work. Nodules less than 3mm are excluded as there is no enough information about their degree of malignancy. The scans are divided into 250 training data and 150 testing data. The LIDC MATLAB toolbox provided by Lampert et al. [29] is used to generate the ground truth data given the XML annotations of the LIDC data as an input. The output of the toolbox includes a separate folder for each slice containing individual masks provided by the four radiologists. The masks are combined together to make Probability Maps (PMaps) where the pixels are summed and normalized to show the Probability of contribution of this pixel to the ground truth nodule according to the radiologists opinions. If the Probability is greater than 0.75 the pixel is counted as a part of the nodule mask. After creating the PMaps, nodules are separated and saved into different matrices for further processing.

B. Preprocessing

Pre-processing helps to provide better visual information for the human eyes, or to get enhanced input for the automated image processing systems. This step reduces noise and artifacts in the lung CT scans. Without preprocessing, it may be difficult to segment the lung parenchyma accurately, locate low-contrast nodules with ground-glass opacity or nodules attached to the blood tree or lung walls [30].

In this stage the scans are sorted then the first and last 8 slices are excluded as they are not showing the internal parts of the lungs. The contrast of the remaining slices is enhanced by first finding the lower and upper intensity limits that can be used for contrast stretching using MATLAB functions. Then the values of the input images are mapped to new values in the enhanced images, between the pre-specified lower and upper limits. Finally, the images are normalized between 0 and 256. An example of the preprocessing output is shown in Fig. 2b.

C. Lung Segmentation

Lung segmentation is one of the important steps in a CAD system. Segmenting the lung areas reduces the running time and minimizes the search space for locating lung nodules. Lung segmentation is necessary as a preprocessing step for the nodule detection to obtain a higher detection rate, and due to similarities between the intensity values of lung wall and nodules. Some obstacles may occur during lung segmentation, such as the nodules connected to the lung wall, which are not considered as a part of the lung parenchyma during the segmentation process. Accuracy, running time, and automation level are used to measure the efficiency a certain technique. In the proposed method, this stage is composed of three main steps: thorax extraction, lung extraction and lung reconstruction.

1) Thorax extraction

This step removes all the external artifacts and air surrounding the patient's body as shown in the original input CT image in Fig. 2a. The algorithm used here is region growing with a technique similar to [31], but instead of using a 2D region growing, a 3D version of it saves much computation time. Also, instead of using four different seed points for each slice, only one seed point is required for the whole scan with coordinates [1,1,1]. The most important part of this step is finding the proper threshold that preserves the lung structure. The greater part of the external area of the thorax is formed of low intensity values. The histogram of the first slice only is analyzed, as in Fig. 3, we can see that there

are two well-defined peaks where the first peak points to the voxels with low intensity that forms the parenchyma and the external region of interest and the second peak points to the lung wall and internal structures. The threshold is calculated as the mid value between the two peaks or the average between them, as explained in Fig. 3. In this step region growing is better than thresholding as it doesn't affect the internal lung parenchyma taking in consideration that it has similar intensity to the thorax external region. The result of this step can be seen in Fig. 2c.

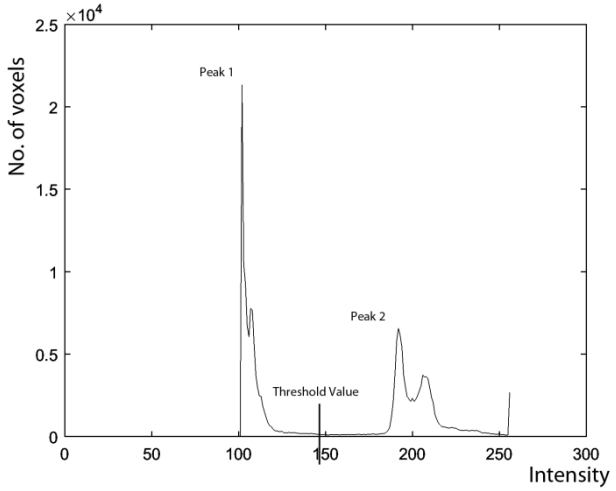

Fig. 3 Example of a CT slice histogram, with threshold value calculated as the average of intensity values of Peak 1 and Peak2

2) Lung extraction

The objective of this step is to separate the lung parenchyma from the surrounding thoracic wall. 3D region growing is also used in this step, but this time to identify high intensity voxels surrounding the lung area. The threshold is calculated in the same way explained in Fig. 3, but the seed point this time is considered as the first non-zero voxel lying on the diagonal line of the first slice in the scan.

Results of lung extraction can be seen in Fig.2d. The output is full of holes because region growing is applied in the 3D space not for each 2D slice. Notice that the nodule connected to the lung wall is excluded from the parenchyma. These errors are corrected in the next step of the lung segmentation.

3) Lung Reconstruction

Some times during the 3D extraction of the lungs, small areas are mistakenly excluded from the pulmonary parenchyma due to intensity similarity with the thoracic wall. These areas can possibly contain nodule candidates connected to the lung walls. So, this stage is very important to reconstruct the edges and preserve peripheral nodule candidates.

To restore the original lung outline, an algorithm similar to the rolling-ball algorithm [31] with some modifications is used. First morphological closing is applied using a circular structure element, with an average radius of 14 pixels, that optimally restores the missing areas without distorting the shape of the lungs or joining both parts of the lungs together. The optimum radius is found through experiments on the provided database. Then a 3D hole filling algorithm is done using a flood-fill operation. Morphological opening is applied to the lung mask again with the same structuring element as the closing to restore the original lung size, and then a logical OR is applied with the lung mask from the previous 'lung extraction' step to restore the sharp edges of the lungs lost through morphological operations. See the results of lung reconstruction is Fig. 2e.

D. Nodule Detection

After narrowing the search space for the nodules in the segmented lungs, next stage in lung cancer CAD systems is the nodule detection. This stage has a high detection sensitivity that locates all the suspicious areas including both the true nodules and a high number of false positives, which can be reduced in the next stages of the CAD system. In a 3D CT scan, a lung nodule is a spherical blob-like object that has a lighter grey-level than the background. Nodules may be separated from other structures, connected to a vessel or connected to the lung wall [32].

Nodule detection is done through two main steps: the first step identifies the internal structure of the lungs that includes both vessels and actual nodules; the second one eliminates the tabular structures to provide nodule candidates.

1) Structure extraction

In this step we work in both 2D and 3D spaces. First, thresholding is applied to each 2D slice to identify the internal high intensity structure and separate it from the lung parenchyma. Calculating the proper threshold isn't as easy as obtaining it in the lung extraction step. There is only one obvious peak in the histogram as there are less number of high intensity areas compared to the other areas. Threshold is obtained as the inflection point of the histogram curve as explained by da silva, et al. [31]. The output of using this threshold contains unwanted edges along the lung walls as in Fig. 4. To remove these artifacts, we first apply canny edge detector to the reconstructed lung mask from the previous steps . Then the edges are dilated with a structuring element of one pixel radius and subtracted from the structure mask. See the results in Fig. 2f.

The next step is to separate each individual 3D structure, to identify nodule candidates. Region growing is applied with seed points chosen from voxels of the structures which has not been reached yet. Due to the large memory overhead, structures are stored in the form of X,Y and Z arrays instead of 3d matrices. The result of 3D structure extraction is shown in Fig. 2g.

2) Tabular Structure Elimination

Sometimes, nodules are attached to the bronchial and vascular trees. This case causes a problem for nodule detection and forces us to identify and eliminate these trees first before

Fig. 4 Edges artifacts of the structure extraction step after thresholding

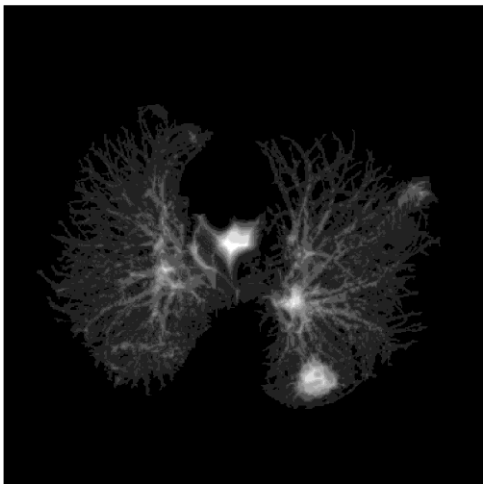

Fig. 5 Depth map calculated with Euclidean distance transform in the tabular structure elimination step

the next stages of the algorithm. Pulmonary vessels have a tabular shape with a very small depth compared to the nodules attached to it, which have a compact round or semi-round shape with larger depth values.

To eliminate tabular vessels, a complete distance transform of the 3D internal structure mask is computed using Euclidean distance, to create a depth map. The Euclidean distance is the straight-line distance between two pixels. For each voxel, the distance transform assigns a number that is the distance between that voxel and the closest nonzero voxel. Nodules -as well as thick lung structures- have distance values up to 6, while vessels and other tabular structures have less distance values. A threshold is set to create the final nodule candidates mask, where all voxels with a distance value greater than 2 is possibly a part of a nodule candidate.

We can see the nodule in the bottom right corner of the depth map presented in Fig.5, along with some other thick pulmonary structures. The result of this stage after applying the threshold can be seen in Fig 2h. Distance transform is applied to all the 3D structures providing us with a list of nodule candidates including a lot of false positives that have to be reduced in the next stages of the algorithm.

E. False Positive Reduction

While the nodule detection step initially identify suspicious nodule candidates, the false-positive reduction step aims to classify the candidates into true nodule and false-positive categories. False positive reduction step aims to achieve maximum sensitivity or true positive rate. Two classifiers are used for this step: A simple Rule-based classifier and Convolutional Neural Networks. But in this paper we only use the Rule-based classifier, keeping CNNs for future work.

The Rule-based classifier works as an initial phase that eliminates the candidates which have more probability Not to be a nodule. it functions through a set of if-then rules with thresholds whose values are chosen carefully through extensive training of the available data set. The rules are applied to a selected set of features that are proven to be more efficient for quickly eliminating the obvious non-nodule candidates. The selected features are: major axis length, minor axis length, area (of the largest slice), volume and spherical disproportion. Nodule volume V is calculated as follows where N is the number of voxels, X is the X-pixel spacing, Y is the Y-pixel spacing and T is the slice thickness:

$$V = N * X * Y * T \quad (1)$$

Spherical disproportion S is the ratio between the dimensions of the bounding box of the object and those of the bounding box of the equivalent sphere. S is calculated as follows where V_B is the volume of the bounding box of the object whose dimensions are obtained by the MATLAB *regionprops* function:

$$S = \frac{V_B}{(2R)^3} \quad (2)$$

where

$$R = \sqrt[3]{\frac{3V}{4\pi}} \quad (3)$$

First, comes the training phase where these features are extracted from the LIDC ground truth nodules. Min and max thresholds of each rule are set as the min and max values of each feature vector. Then the same set of features are extracted from each candidate during the testing phase making a vector that characterizes them, and fed to the Rule-based classifier. Results of the used classifier are shown in Fig.6. This classifier is an initial step for intensive classification using CNNs or Support Vector Machines (SVM).

IV. Results and Discussion

In this section, we present the results obtained with the proposed algorithm for the detection of pulmonary nodules. The images used here are obtained from the LIDC dataset with

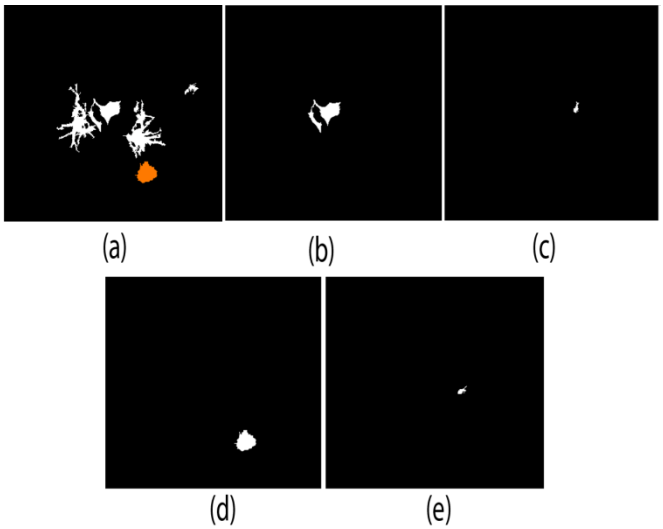

Fig. 6 Example for nodule candidates provided by the Rule-based Classifier. (a) The output of the tabular structure elimination step. Notice the actual only nodule in (d). (b), (c) and (e) are false positives.

a total of 250 training data and 150 testing data. Number of nodules in the testing data are 262 nodules. Thresholds obtained through the training dataset are detailed in Table1.

TABLE 1 Thresholds of the Rule-based classifier

Feature	**Min Threshold**	**Max Threshold**
Major axis length	1.2	52.1005
Minor axis length	1.154	40.8242
Area	11	1645
Volume	1.948	22708.297
Spherical Disproportion	0.5236	15.1616

In order to evaluate the efficiency of the algorithm, sensitivity, specificity and accuracy are considered. Sensitivity is defined as the true positive rate: TP / (TP + FN), specificity is the true negative rate: TN / (TN + FP) and the accuracy of the CAD system is the rate of both: (TP + TN) / (TP + TN + FP + FN), where TP is the number of actual nodules found correctly, TN is the number of non-nodules correctly excluded, FP is the number of non-nodule structures considered as nodules and FN is the number of missed nodules.

The total sensitivity of the algorithm measured on the testing data is 77.77%, specificity is 69.5% and accuracy is 70.53 % with an average of 4.1 FPs/scan. The results are satisfactory taking in consideration that the simple Rule-based classifier used was only an initial first step of the classification and FP reduction. The time required to run the algorithm varies from a case to another, depending on the number of slices of each scan. Average running time is estimated as 127.96 seconds on an Intel core i7 CPU with 8 GB RAM.

Comparatively, the authors in [31] achieved a total sensitivity of 84.84 % and 96.15% specificity using Support Vector Machine classifier on a 33 input scans. In [16] the algorithm achieved a total sensitivity of 82.66% with 3 FPs/scan using two classifiers and a dataset of 84 scans. Sivakumar, et al. [33] achieved a total accuracy of 80.36%, specificity of 76.47% and sensitivity of 82.05% using a dataset of 54 scans. The authors in [34] used a Rule-based classifier on 90 scans achieving a total detection rate of 85% with 2 FPs/scan.

V. Conclusion

Designing an efficient and complete lung CAD system is very important as early detection of lung nodules can improve the effectiveness of treatment and increase the patient's chances of survival. This paper proposes a fully automated algorithm that is based on simple and quick steps, which produce consistent output for the same inputs. Most of the steps are done in the 3D space to preserve the 3D characteristics of the detected nodules. For thorax and lung segmentation, 3D Region Growing is used to segment regions of interest. The missing parts of the lungs are reconstructed using morphological operations and 3D hole filling algorithms. Internal lung structures are extracted using 2D thresholding and 3D Region Growing. Nodule candidates are detected by excluding tabular structures, which is done by building a complete depth map using Euclidean distance transform. Finally, a simple Rule-based Classifier is designed to preserve the most qualified nodule candidates. The features used in the classifier are chosen carefully among tens of available features for lung nodules through extensive experiments. This classifier works only as an initial classification step that achieved a total sensitivity of 77.77%, specificity of 69.5% and a total accuracy of 70.53%. The algorithm can easily detect well-circumscribed nodules as well as nodules attached to the lung wall or to lung vessels. Some ground glass nodules cannot be detected using our CAD system due to their high transparency.

In future work we will focus on building an efficient classifier using SVM or CNNs to reduce the numbers of FPs and increase the overall accuracy of the algorithm. Also, we will try to test the algorithm on more datasets along with the rest of the LIDC database.

References

[1] A. Jemal, R. Siegel, E. Ward, Y. Hao, J. Xu, and M. J. Thun, "Cancer statistics," CA. Cancer J. Clin., vol. 59, no. 4, pp. 225–49, January, 2009.

[2] A. El-Baz and J. S. Suri, Lung Imaging and Computer Aided Diagnosis. CRC Press, pp. 189–219, 2011.

[3] J. Austin, N. Müller, and P. Friedman, "Glossary of terms for CT of the lungs: recommendations of the Nomenclature Committee of the Fleischner Society.," Radiology, no. 200, pp. 327–331, 1996.

[4] T. Way, H. Chan, L. Hadjiiski, and B. Sahiner, "Computer-Aided Diagnosis of Lung Nodules on CT Scans:: ROC Study of Its Effect on Radiologists' Performance," Acad. Radiol., no. 3, pp. 323–332, 2010.

[5] S. K. Shah et al., "Solitary pulmonary nodule diagnosis on CT: results of an observer study.," Acad. Radiol., vol. 12, no. 4, pp. 496–501, April 2005.

[6] I. Sluimer, A. Schilham, M. Prokop, and B. Van Ginneken, "Computer analysis of computed tomography scans of the lung: A

survey," IEEE Trans. Med. Imaging, vol. 25, no. 4, pp. 385–405, 2006.

[7] A. El-Baz et al., "Computer-aided diagnosis systems for lung cancer: Challenges and methodologies," Int. J. Biomed. Imaging, vol. 2013, 2013.

[8] U. Bağcı, M. Bray, J. Caban, J. Yao, and D. J. Mollura, "Computer-assisted detection of infectious lung diseases: A review," Comput. Med. Imaging Graph., vol. 36, pp. 72–84, 2012.

[9] S. L. a Lee, a. Z. Kouzani, and E. J. Hu, "Automated detection of lung nodules in computed tomography images: A review," Mach. Vis. Appl., vol. 23, pp. 151–163, 2012.

[10] K. Devaki and V. Muralibhaskaran, "Study of computed tomography images of the lungs: A survey," Int. Conf. Recent Trends Inf. Technol. ICRTIT 2011, pp. 837–842, 2011.

[11] I. R. S. Valente, P. C. Cortez, E. C. Neto, J. M. Soares, V. H. C. de Albuquerque, and J. M. R. S. Tavares, "Automatic 3D pulmonary nodule detection in CT images: A survey," Comput. Methods Programs Biomed., vol. 124, no. February, pp. 91–107, 2016.

[12] B. K and S. M.V, "Techniques for Detection of Solitary Pulmonary Nodules in Human Lung and Their Classifications -A Survey," Int. J. Cybern. Informatics, vol. 4, no. 1, pp. 27–40, 2015.

[13] H. Mahersia and M. Zaroug, "Lung Cancer Detection on CT Scan Images : A Review on the Analysis Techniques," vol. 4, no. 4, pp. 38–45, 2015.

[14] S. A. El-Regaily, M. A. Salem, and M. H. Abdel Aziz, "Survey of Computer Aided Detection Systems for Lung Cancer in Computed Tomography," Curr. Med. Imaging Rev., vol. 13, June 2017.

[15] M. A. Salem, "Recent Survey on Medical Image Segmentation," in Handbook of Research on Machine Learning Innovations and Trends, no. 1953, IGI Global, pp. 424–464, 2017.

[16] T. Messay, R. C. Hardie, and S. K. Rogers, "A new computationally efficient CAD system for pulmonary nodule detection in CT imagery," Med. Image Anal., vol. 14, no. 3, pp. 390–406, 2010.

[17] M. Tan, R. Deklerck, B. Jansen, M. Bister, and J. Cornelis, "A novel computer-aided lung nodule detection system for CT images," Med. Phys., vol. 38, no. 10, p. 5630, 2011.

[18] M. E. Fantacci et al., "Algorithms for automatic detection of lung nodules in CT scans," Plateau, vol. 5, pp. 8–12, 2011.

[19] X. Ye, X. Lin, J. Dehmeshki, G. Slabaugh, and G. Beddoe, "Shape-based computer-aided detection of lung nodules in thoracic CT images," IEEE Trans. Biomed. Eng., vol. 56, no. 7, pp. 1810–1820, 2009.

[20] V. Kuppusamy, "Feature Extraction Based Lung Nodule Detection in CT Images," Int. J. Appl. Eng. Res., vol. 11, no. 4, pp. 2697–2700, 2016.

[21] A. O. de Carvalho Filho, A. C. Silva, A. C. de Paiva, R. A. Nunes, and M. Gattass, "Computer-aided diagnosis system for lung nodules based on computed tomography using shape analysis, a genetic algorithm, and SVM," Med. Biol. Eng. Comput., pp. 1–18, 2016.

[22] Z. Abduh, M. A. Wahed, and Y. M. Kadah, "Robust Computer-Aided Detection of Pulmonary Nodules from Chest Computed Tomography," J. Med. Imaging Heal. Informatics, vol. 6, no. 3, pp. 693–699, 2016.

[23] Q. Dou, H. Chen, L. Yu, J. Qin, and P. A. Heng, "Multi-level Contextual 3D CNNs for False Positive Reduction in Pulmonary Nodule Detection," IEEE Trans. Biomed. Eng., pp. 1–1, 2016.

[24] W. Sun, B. Zheng, and W. Qian, "Computer aided lung cancer diagnosis with deep learning algorithms," SPIE Med. Imaging, vol. 9785, p. 97850Z–97850Z–8, 2016.

[25] N. Duggan et al., "A Technique for Lung Nodule Candidate Detection in CT Using Global Minimization Methods," Energy Minimization Methods Comput. Vis. Pattern Recognit., pp. 478–491, 2015.

[26] M. F. McNitt-Gray et al., "The Lung Image Database Consortium (LIDC) Data Collection Process for Nodule Detection and Annotation," Acad. Radiol., vol. 14, no. Lidc, pp. 1464–1474, 2007.

[27] S. G. Armato et al., "The Lung Image Database Consortium (LIDC) and Image Database Resource Initiative (IDRI): a completed reference database of lung nodules on CT scans.," Med. Phys., vol. 38, no. February, pp. 915–931, 2011.

[28] A. P. Reeves et al., "The Lung Image Database Consortium (LIDC). A Comparison of Different Size Metrics for Pulmonary Nodule Measurements," Acad. Radiol., vol. 14, no. Lidc, pp. 1475–1485, 2007.

[29] T. a. Lampert, A. Stumpf, and P. Gançarski, "An Empirical Study Into Annotator Agreement, Ground Truth Estimation, and Algorithm Evaluation," IEEE Trans. Image Process., vol. 25, no. 6, pp. 2557–2572, 2016.

[30] A. Chaudhary and sukhraj sonit, "Volume 2 , Issue 2 (February 2012) ISSN : 2249-3905 lung cancer detection using digital image processing ijreas Volume 2 , Issue 2 (February 2012) ISSN : 2249-3905," vol. 2, no. 2, pp. 1351–1359, 2012.

[31] J. R. F. D. S. Sousa, A. C. Silva, A. C. de Paiva, and R. A. Nunes, "Methodology for automatic detection of lung nodules in computerized tomography images.," Comput. Methods Programs Biomed., vol. 98, pp. 1–14, 2010.

[32] S. Diciotti, G. Picozzi, M. Falchini, M. Mascalchi, N. Villari, and G. Valli, "3-D segmentation algorithm of small lung nodules in spiral CT images.," IEEE Trans. Inf. Technol. Biomed., vol. 12, no. 1, pp. 7–19, 2008.

[33] S. Sivakumar, C. Chandrasekar, and A. L. Cancer, "Lung Nodule Detection Using Fuzzy Clustering and Support Vector Machines," vol. 5, no. 1, pp. 179–185, 2013.

[34] T. Jia, Y. Wei, and C. D. Wu, "A lung cancer lesions dectection scheme based on CT image," ICSPS 2010 - Proc. 2010 2nd Int. Conf. Signal Process. Syst., vol. 1, no. 3, pp. 557–560, 2010.